Journal of Colloid and Interface Science 328 (2008) 196–202

Contents lists available at ScienceDirect

Journal of Colloid and Interface Science

www.elsevier.com/locate/jcis

Cononsolvency-induced micellization kinetics of pyrene end-labeled diblock copolymer of *N*-isopropylacrylamide and oligo(ethylene glycol) methyl ether methacrylate studied by stopped-flow light-scattering and fluorescence

Jingyi Rao, Jingyan Zhang, Jian Xu, Shiyong Liu *

Key Laboratory of Soft Matter Chemistry, Department of Polymer Science and Engineering, Hefei National Laboratory for Physical Sciences at the Microscale, University of Science and Technology of China, Hefei, Anhui 230026, China

ARTICLE INFO

Article history:
Received 27 April 2008
Accepted 1 September 2008
Available online 4 September 2008

Keywords:
Cononsolvency
Fluorescence
Stopped-flow
Kinetics
Transient micelles
Block copolymer

ABSTRACT

Cononsolvency-induced micellization kinetics of a pyrene end-labeled diblock copolymer of *N*-isopropylacrylamide and oligo(ethylene glycol) methyl ether methacrylate, *Py*-PNIPAM-*b*-POEGMA, was investigated in detail via a combination of stopped-flow light-scattering and fluorescence techniques. Upon a stopped-flow jump from pure methanol to proper methanol/water mixtures, scattered light intensity exhibited an initial increase and then stabilized out; whereas the time-dependence of monomer to excimer fluorescence intensity ratios (I_E/I_M) revealed an abrupt increase followed by a gradual decrease to plateau values. The dynamic traces of scattered intensity can be well fitted by double exponential functions, the obtained $\tau_{1,scat}$ and $\tau_{2,scat}$ can be ascribed to processes of forming quasi-equilibrium micelles and their relaxation into final equilibrium states, respectively. On the other hand, a triple exponential function was needed to fit the dynamic traces of I_E/I_M, leading to three characteristic relaxation times ($\tau_{1,fluo}$, $\tau_{2,fluo}$, and $\tau_{3,fluo}$). It was found that the time scales of $\tau_{1,scat}$ and $\tau_{2,scat}$ obtained from stopped-flow light scattering were in general agreement with $\tau_{2,fluo}$ and $\tau_{3,fluo}$ obtained from stopped-flow fluorescence. Considering that excimer fluorescence is extremely sensitive to small aggregates, the newly detected fast process ($\tau_{1,fluo} \sim 10$ ms) by stopped-flow fluorescence should be ascribed to the early stage of micellization, i.e., the burst formation of small transient micelles, in which light scattering detection was still not sensitive enough. These small transient micelles fused and grew into quasi-equilibrium micelles, which then slowly relaxed into the final equilibrium state.

1. Introduction

In recent decades, considerable attention has been drawn to block copolymer self-assembly in selective solvents due to their promising applications such as targeted drug delivery and catalysis [1–3]. Self-assembled aggregates of various morphologies have been reported, ranging from spherical micelles to vesicles, tubules, and complex super-aggregates, which can be well tuned by the relative block length, solvent composition, polymer concentration, additives, and temperature [4–12]. However, most of the past studies of block copolymer micelles have focused on the characterization of their equilibrium structures [13–19], and less attention has been paid to self-assembling process and the underlying kinetics.

Like small molecule surfactants, the micellization kinetics of block copolymers is closely related to their stability, which plays an important role in various technological processes. For block copolymers, the characteristic relaxation time for a copolymer chain to escape from the micelles has been theoretically considered by Halperin and Alexander on the basis of scaling analysis within the context of Aniansson and Wall (A–W) theory developed for surfactants [20–23]. They concluded that the insertion/expulsion of individual chains (unimer exchange) is the only mechanism for the micelle relaxation process upon small perturbation from equilibrium state. It should be noted that this conclusion is only valid for small deviations from the initial equilibrium state. Temperature jump (typically $\Delta T = 1$–$2\,^{\circ}C$) experiments with light scattering detection are suitable to verify the proposed micellization dynamics. Water-soluble poly(ethylene oxide)-*b*-poly(propylene oxide)-*b*-poly(ethylene oxide) (PEO-*b*-PPO-*b*-PEO) triblock copolymers, Pluronics, have been exclusively selected for this purpose [24–28].

For large perturbations, such as unimer-to-micelle transition, Mattice et al. [29] performed computer simulations, suggesting the presence of two processes with different time scales, the unimer concentration drops close to the critical micellization concentration (CMC) very quickly in the fast process, followed by the

* Corresponding author. Fax: +86 551 3607348.
E-mail address: sliu@ustc.edu.cn (S. Liu).

0021-9797/$ – see front matter
doi:10.1016/j.jcis.2008.09.001

step approaching the equilibrium state at a much slower rate. Dormidontova and co-workers [30–32] further proposed a micelle fusion/fission–unimer expulsion/entry joint mechanism for block copolymer micelle evolution, suggesting that micelle fusion/fission dominates over unimer entry/expulsion in the initial fast process; while the latter mechanism dominates during the second slow process. Nyrkova and Semenov [33,34] recently postulated that the unimer-to-micelle transition cannot be simply characterized by just two relaxation times, but rather by a continuous spectrum of relaxation times. They also proposed that the main route of micelle growth should involve step-by-step joining of unimers, i.e., insertion/expulsion of individual chains. Thus, whether micelle fusion/fission mechanism plays a key role in micelle growth has been a matter of debate.

Recently, we reported the kinetics of pH-induced micellization of a stimulus-responsive ABC triblock copolymer, namely poly(glycerol monomethacrylate)-*b*-poly(2-(dimethylamino)ethyl methacrylate)-*b*-poly(2-(diethylamino)ethyl methacrylate) (PGMA-*b*-PDMA-*b*-PDEA) [35]. The micellization kinetics was investigated by stopped-flow light scattering and analyzed in the context of Dormidontova theory. We also studied the micellar formation and inversion kinetics of a schizophrenic diblock copolymer of poly(4-vinylbenzoic acid)-*b*-poly(*N*-(morpholino)ethyl methacrylate) (PVBA-*b*-PMEMA), induced by a combination of pH and ionic strengths [36]. However, though several kinetic studies have been conducted, more systems with different characteristics should be needed to reach a general consensus concerning the micellization kinetics.

We previously reported the first example of cononsolvency-induced micellization of a pyrene end-labeled diblock copolymer, poly(*N*-isopropylacrylamide)-*b*-poly(oligo(ethylene glycol) methyl ether methacrylate) (*Py*-PNIPAM-*b*-POEGMA) [37]. It should be noted that cononsolvency is a modestly rare phenomenon, in which a mixture of two good solvents for a polymer becomes a nonsolvent [38–41]. Originally reported by Schild et al. [39,41], poly(*N*-isopropylacrylamide) (PNIPAM) exhibits such rare solution properties in an appropriate mixture of water and polar organic solvents, such as methanol, ethanol, tetrahydrofuran, or 1,4-dioxane. The cononsolvency-induced PNIPAM-core micelles from *Py*-PNIPAM-*b*-POEGMA in methanol/water mixture have been characterized by ^{1}H NMR, laser light scattering (LLS), fluorescence spectroscopy, and transmission electron microscopy [37].

We have also investigated the cononsolvency-induced micellization process of *Py*-PNIPAM-*b*-POEGMA in methanol/water mixture by monitoring the time-dependent evolution of fluorescence spectra. It was found that the excimer to monomer fluorescence intensity ratios, I_E/I_M, continuously decreased with time and stabilized out within ~20 min [37]. We ascribed the observed process to the structural arrangement and further packing of PNIPAM segments within the micelle core after the initial formation of pseudo-equilibrium micelles. However, kinetic information of the early stage events during the cononsolvency-induced micellization was still missing due to that the first fluorescence spectrum can only be obtained ~5 s after mixing the copolymer solution in methanol with water.

To obtain a whole picture of the micellization processes and elucidate the underlying mechanism, herein, we further investigated the cononsolvency-induced micellization kinetics of *Py*-PNIPAM-*b*-POEGMA via the stopped-flow technique, which can provide kinetic information with time resolutions down to a few milliseconds due to its fast and efficient mixing within ~1 ms. A combination of in-situ time-resolved light scattering and fluorescence detections enabled a detailed exploration of early stage micellization kinetics.

2. Materials and methods

2.1. Materials

Poly(*N*-isopropylacrylamide)-*b*-poly(oligo(ethylene glycol) methyl ether methacrylate), *Py*-PNIAPM-*b*-POEGMA, was synthesized via sequential reversible addition-fragmentation chain transfer (RAFT) polymerization of *N*-isopropylacrylamide (NIPAM) and oligo(ethylene glycol) methyl ether methacrylate (OEGMA, M_n = 475, mean degree of polymerization, DP, is ~8–9) monomers using a pyrene-containing dithioester as the RAFT agent. Detailed experimental procedures were reported previously [37]. The DPs of PNIPAM and POEGMA blocks were determined to be 50 and 18 by ^{1}H NMR in $CDCl_3$, respectively. The obtained diblock copolymer was denoted *Py*-PNIPAM$_{50}$-*b*-POEGMA$_{18}$. The molecular weight and molecular weight distributions were characterized by GPC analysis in THF: $M_n = 14{,}500$, $M_w/M_n = 1.09$.

2.2. Characterization

Stopped-flow studies are carried out using a Bio-Logic SFM300/S stopped-flow instrument. It is equipped with three 10 mL step-motor-driven syringes (S1, S2, and S3), which can be operated independently to carry out single- or double-mixing. The stopped-flow device is attached to a MOS-250 spectrometer; kinetic data were fitted using the Biokine program provided by Bio-Logic. For the light scattering detection at a scattering angle of 90°, both the excitation and emission wavelengths were adjusted to 335 nm with 10 nm slits. While for the fluorescence detection, the excitation wavelength was set at 338 nm, and the emission wavelengths were respectively set at 373 and 480 nm to record the time-dependence of intensity of the monomer and excimer fluorescence. 5 nm slits were always used for both the excitation and emission monochromator. Using FC-15 flow cell, typical dead time is 2.6 ms, respectively. Temperature was maintained at 25 °C by circulating water around the syringe chamber and observation head.

3. Results and discussion

3.1. Stopped-flow light-scattering results

In pure methanol or water, *Py*-PNIPAM$_{50}$-*b*-POEGMA$_{18}$ molecularly dissolves [37]. Due to the cononsolvency behavior of PNIPAM block, it can self-assemble into PNIPAM-core micelles stabilized with POEGMA corona in an appropriate range of methanol/water mixture. We employed stopped-flow to study the cononsolvency-induced micellization kinetics, especially at the early stages. The double-mixing setup of stopped-flow allows the convenient and independent changes of solvent compositions or polymer concentrations. The time resolution is limited by the dead time of the stopped-flow apparatus, which can be down to 1–3 ms.

Fig. 1 shows the time dependence of scattered light intensity upon a jump of the volume fraction of water, φ_{water}, from 0 to different final values by stopped-flow mixing *Py*-PNIPAM$_{50}$-*b*-POEGMA$_{18}$ in methanol with different volumes of water. At $\varphi_{water} < 0.47$ and > 0.8, the dynamic traces of scattered light intensity remain as straight lines and no relaxation processes can be discerned (Fig. 1a), indicating that the diblock copolymer remains molecularly soluble.

At $\varphi_{water} = 0.47$ (Fig. 1b), the scattered light intensity reveals an abrupt increase within the first ~1 s and then reaches a plateau value. This indicates that the solubility of PNIPAM block is getting worse due to cononsolvency and aggregation between diblock copolymer chains, leading to the formation of PNIPAM-core micelles with possibly loose structures. At φ_{water} of 0.5–0.67, we

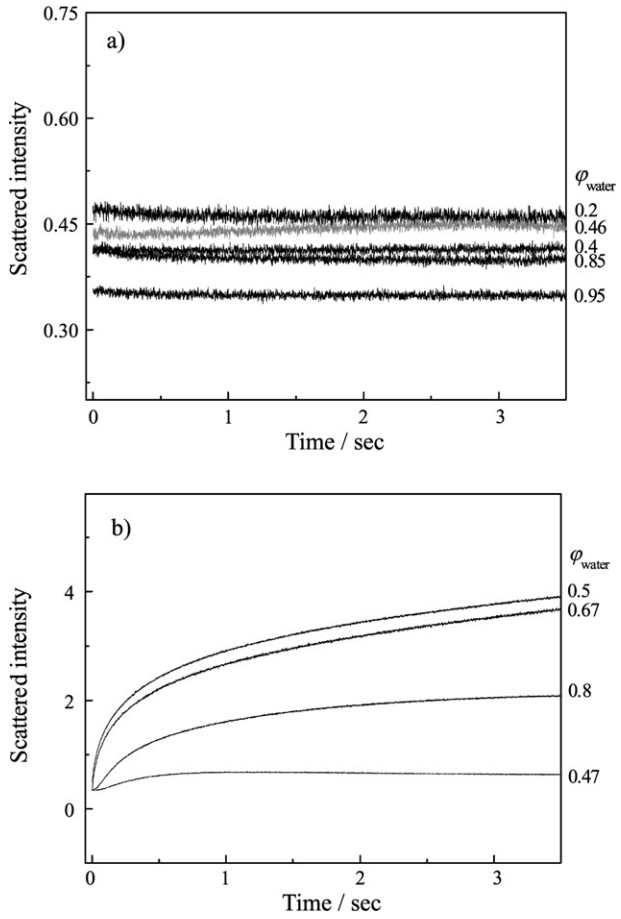

Fig. 1. Time dependence of scattered light intensity upon stopped-flow mixing *Py*-PNIPAM$_{50}$-*b*-POEGMA$_{18}$ solution in methanol with water. The volume fraction of water, φ_{water}, was varied and the final copolymer concentration was fixed at 1.0 g/L.

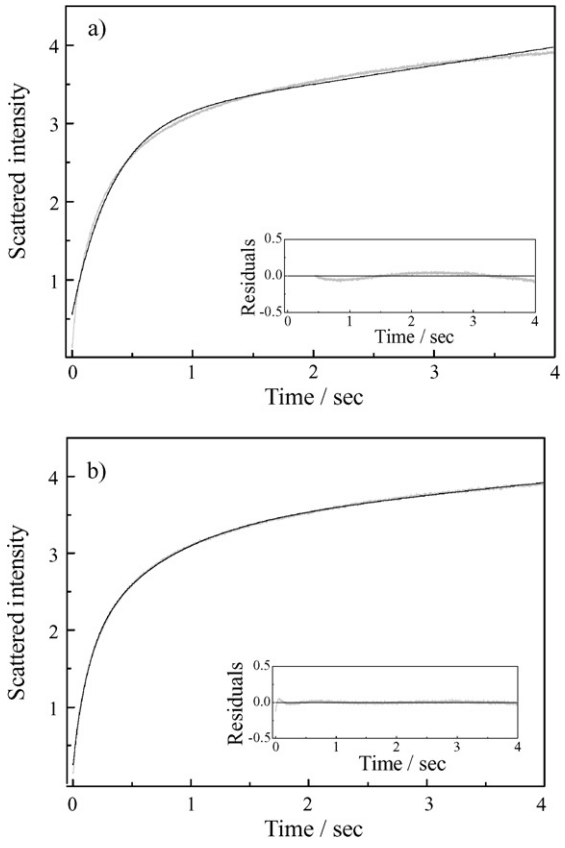

Fig. 2. Typical time dependence of the scattered light intensity recorded during micelle formation. The upper and lower figures were fitted by (a) single- and (b) double-exponential functions, respectively. The final *Py*-PNIPAM$_{50}$-*b*-POEGMA$_{18}$ diblock copolymer concentration was 1.0 g/L and $\varphi_{water} = 0.5$.

can observe a relaxation process with quite large positive amplitude, and the final scattered light intensity exhibits a maximum at $\varphi_{water} = 0.5$. At a final φ_{water} of 0.8, the scattered light intensity shows a relatively quick increase initially, followed by a more gradual increase. The above results reveal that the cononsolvency-induced formation of PNIPAM-core micelles occurs in the φ_{water} range of 0.47–0.8. This is in general agreement with the cononsolvency behavior of PNIPAM homopolymer [38,40] and our previous investigation [37].

It should be noted that in Fig. 1, the scattered light intensity of all dynamic traces at $t = 0$ remains nearly the same, which is different from the pH-responsive micellization kinetics of PGMA-*b*-PDMA-*b*-PDEA [35]. The absence of intensity loss within the stopped-flow dead time (1–2 ms) suggests that the cononsolvency-induced micellization of *Py*-PNIPAM$_{50}$-*b*-POEGMA$_{18}$ is much slower as compared to that of pH-induced micellization. We can thus monitor the whole relaxation process of cononsolvency-induced micellization using the stopped-flow technique.

In the previous report [37], we have established by laser light scattering (LLS) that at $\varphi_{water} = 0.5$, the formed PNIPAM-core micelles possess the largest average aggregation number per micelle, N_{agg}, and overall micelle density (ρ). Indeed, in Fig. 1b, the final scattered light intensity value at $\varphi_{water} = 0.5$ is the largest within the φ_{water} range investigated. Subsequent kinetic studies then focus on this specific case, i.e., $\varphi_{water} = 0.5$.

The time dependence of the scattered light intensity I_t can be converted to a normalized function, namely, $(I_\infty - I_t)/I_\infty$ versus t, where I_∞ is the value of I_t at an infinitely long time [42]. Typical fitting results of the time dependence of the scattered light intensity at $\varphi_{water} = 0.5$ are shown in Fig. 2.

In agreement with those previously reported for the pH-induced micellization kinetics of PGMA-*b*-PDMA-*b*-PDEA [35], single exponential function cannot fit the relaxation curve (Fig. 2a). Empirically, we found that such a function could be well fitted by a double exponential function (Fig. 2b)

$$(I_\infty - I_t)/I_\infty = c_1 e^{-t/\tau_1} + c_2 e^{-t/\tau_2}, \quad (1)$$

where c_1 and c_2 are the normalized amplitudes ($c_2 = 1 - c_1$). τ_1 and τ_2 are the characteristic relaxation time of two processes, $\tau_1 < \tau_2$, and they are denoted as $\tau_{1,scat}$ and $\tau_{2,scat}$, respectively. The mean relaxation time for the overall micelle formation, $\tau_{f,scat}$, can be calculated as

$$\tau_{f,scat} = c_1\tau_{1,scat} + c_2\tau_{2,scat}. \quad (2)$$

Both processes associated with $\tau_{1,scat}$ and $\tau_{2,scat}$ possess positive amplitudes. At a final φ_{water} of 0.5 and a copolymer concentration of 1.0 g/L, $\tau_{1,scat}$ and $\tau_{2,scat}$ are 0.12 s and 0.98 s, respectively.

Following the Dormidontova model of the unimer-to-micelle transition, the fast process ($\tau_{1,scat}$) is ascribed to the quick association of unimers into a large amount of small micelles and their subsequent growth into quasi-equilibrium micelles [30]. The aggregation number N_{agg} abruptly increases during this process, leading to fast changes of scattered intensity. At the end of the fast process, the unimer concentration decreases close to CMC. The slow process ($\tau_{2,scat}$) should be ascribed to relaxation of the number of micelles involving micelle formation/breakup, approaching the final equilibrium state. However, the slow process (micelle formation/breakup) can proceed via unimer insertion/expulsion or micelle fusion/fission.

To elucidate the underlying mechanism, we further investigated the copolymer concentration dependence of $\tau_{1,\mathrm{scat}}$ and $\tau_{2,\mathrm{scat}}$ at $\varphi_{\mathrm{water}} = 0.5$ (Fig. 3). If the final copolymer concentration is $\leqslant$0.2 g/L, we do not observe any relaxation of scattered intensity. Above 0.2 g/L, relaxation processes with positive amplitudes are typically observed. All the dynamic traces in Fig. 3 can be well-fitted with a double exponential function and the results are shown in Fig. 4. $\tau_{1,\mathrm{scat}}$ is in the range of 0.1–0.35 s, and $\tau_{2,\mathrm{scat}}$ is in the range 1.0–1.8 s. Both of them decrease with increasing copolymer concentrations.

Dormidontova [30] theoretically predicted that fusion between small micelles will dominate over the unimer insertion/expulsion to form quasi-equilibrium micelles. As we can see from Fig. 4, $\tau_{1,\mathrm{scat}}$ decreases with increasing polymer concentration, which strongly suggests that the relaxation from the initially formed small micelles to the quasi-equilibrium micelles mainly proceeds via micelle fusion/fission. The slow process (τ_2) is associated with micelle formation/breakup, leading to micelles of larger aggregation numbers and lower number densities. Here, $\tau_{2,\mathrm{scat}}$ decreases with increasing copolymer concentration, which suggests that the associated slow micelle formation/breakup process also proceeds via the micelle fusion/fission mechanism. It should be noted that in the above arguments, the formation of large amounts of small transient micelles lacks direct experimental evidence, partially due to that the scattered intensity at a scattering angle of 90° is insensitive to the small variations of N_{agg}.

3.2. Stopped-flow fluorescence kinetics

Excimer fluorescence technique can provide highly local information due to that the excimer is only formed when two aromatic rings closely approach to each other (within 4–5 Å) [43–50]. Thus, the variation of excimer fluorescence intensity can provide sensitive information about the formation of small aggregates, as long as the average N_{agg} is $\geqslant$2. Pyrene has been successfully employed as a probe of helix–helix proximity and protein conformational changes, depending on the ability of two pyrene molecules coming into contact [43–45,50,51]. The latter is mainly determined by the chain mobility and local concentrations. Thus, pyrene end-labeled diblock copolymer, *Py*-PNIPAM$_{50}$-*b*-POEGMA$_{18}$, used in this study provides to be a suitable system to investigate the aggregation kinetics at the very early stages.

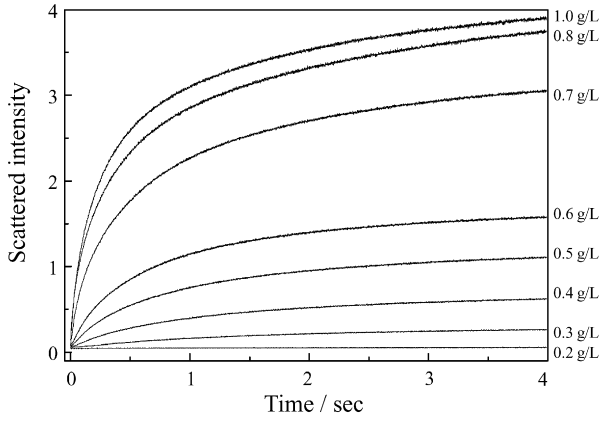

Fig. 3. Time dependence of scattered light intensity upon stopped-flow mixing the methanol solution of *Py*-PNIPAM$_{50}$-*b*-POEGMA$_{18}$ with equal volume of water at 25 °C. From bottom to top, the final polymer concentrations were 0.2, 0.3, 0.4, 0.5, 0.6, 0.7, 0.8 and 1.0 g/L, respectively.

The fluorescence emission spectra of *Py*-PNIPAM$_{50}$-*b*-POEGMA$_{18}$ micelles in the φ_{water} range of 0.47–0.8 typically exhibit three distinct peaks at 373, 393, and 415 nm, and the excimer emission of pyrene appears as a broad, structureless band around 480 nm. Using the monomer emission intensity at 373 nm as a reference, the spectral parameter of interest to us is the excimer (480 nm) to monomer (373 nm) intensity ratios, $I_{\mathrm{E}}/I_{\mathrm{M}}$.

Fig. 5 shows the time dependence of $I_{\mathrm{E}}/I_{\mathrm{M}}$ of *Py*-PNIPAM$_{50}$-*b*-POEGMA$_{18}$ at different final φ_{water} by stopped-flow mixing the copolymer solution in methanol with water. The φ_{water} range (0.47–0.8) in which the variation of $I_{\mathrm{E}}/I_{\mathrm{M}}$ with time can be discerned generally agree with those obtained from stopped-flow light scattering. An exception occurs for $\varphi_{\mathrm{water}} = 0.46$, although stopped-flow light scattering reveals no relaxation process, the time dependence of $I_{\mathrm{E}}/I_{\mathrm{M}}$ exhibits a sharp decrease within the initial ~1 s. As the final plateau $I_{\mathrm{E}}/I_{\mathrm{M}}$ value is consistent with other traces (Fig. 5a), we believe that the abnormal relaxation behavior of $I_{\mathrm{E}}/I_{\mathrm{M}}$ at $\varphi_{\mathrm{water}} = 0.46$ should be ascribed to the slight aggregation of copolymer chains immediately after the solvent jump.

At $\varphi_{\mathrm{water}} = 0.47$ (Fig. 5b), stopped-flow fluorescence kinetic studies reveal that $I_{\mathrm{E}}/I_{\mathrm{M}}$ increases within the initial ~0.3 s and then stabilizes out. In the final φ_{water} range of 0.5–0.8, dynamic traces of $I_{\mathrm{E}}/I_{\mathrm{M}}$ exhibit a burst increase upon stopped-flow mixing and then slowly decrease at extended time periods. Previous static fluorescence results have revealed that equilibrium $I_{\mathrm{E}}/I_{\mathrm{M}}$ value exhibits a maximum at $\varphi_{\mathrm{water}} = 0.67$ although PNIPAM-core micelles formed at $\varphi_{\mathrm{water}} = 0.5$ possess the highest overall micelle density and apparent molar mass [37]. This is further confirmed by stopped-flow fluorescence results. From Fig. 5b, we can see that the final $I_{\mathrm{E}}/I_{\mathrm{M}}$ value at $\varphi_{\mathrm{water}} = 0.67$ within the stopped-flow time window is larger than that at $\varphi_{\mathrm{water}} = 0.50$.

The different kinetic traces of scattered intensity and $I_{\mathrm{E}}/I_{\mathrm{M}}$ in the final φ_{water} range of 0.47–0.8 suggest that these two detection techniques report different aspects concerning the micellization kinetics. According to the typical fitting results of the time dependence of scattered light intensity at $\varphi_{\mathrm{water}} = 0.5$, two sequential relaxation processes are probed. The fast relaxation process ($\tau_{1,\mathrm{scat}} = 0.12$ s) is associated with quite large positive amplitudes ($c_1 = 0.61$). As a large increase of N_{agg} is involved, this fast process should be ascribed to the transformation of unimers into quasi-

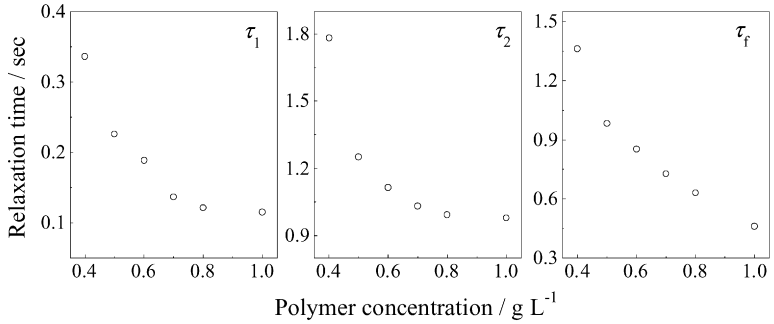

Fig. 4. Double-exponential fitting results of the time-dependence of scattered light intensity during micelle formation at various *Py*-PNIPAM$_{50}$-*b*-POEGMA$_{18}$ concentrations. The experimental conditions were the same as those described in Fig. 3.

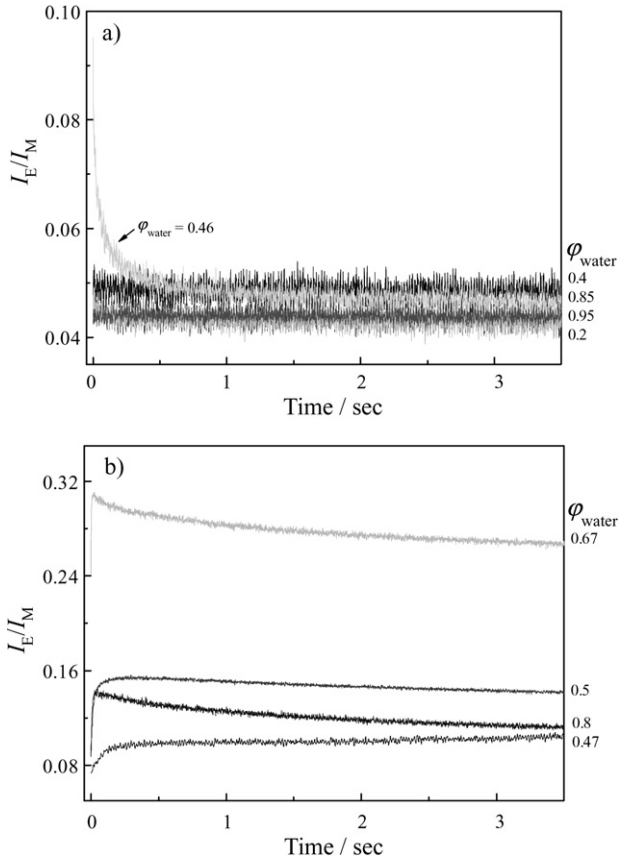

Fig. 5. Time dependence of the ratio of excimer to monomer fluorescence emission intensity (I_E/I_M) upon stopped-flow mixing the *Py*-PNIPAM$_{50}$-*b*-POEGMA$_{18}$ solution in methanol with water. The final φ_{water} was varied and the copolymer concentrations were fixed at 1.0 g/L.

equilibrium micelles, which possibly passes through a transient stage, i.e., the formation of large amounts of small micelles. The second slow process ($\tau_{2,scat} = 0.98$ s) is associated with relatively small positive amplitudes ($c_{2,scat} = -0.39$), in which micelle formation/breakup occurs and the system comes close to the final equilibrium state.

As the scattered light intensity at 90° is insensitive to the small variation of N_{agg}, it will not be able to detect the early stage process associated with the formation of small transient micelles. On the other hand, excimer fluorescence intensity should be quite powerful in detecting the presence of intermediate small aggregates. Moreover, for *Py*-PNIPAM$_{50}$-*b*-POEGMA$_{18}$ solution in pure methanol or water, the excimer fluorescence peaks were very weak, indicating the absence of any pre-association between terminal pyrene groups and that diblock copolymer dissolved as unimer chains [37]. Thus, the time-dependent increase of I_E/I_M after stopped-flow mixing should be ascribed to cononsolvency-induced aggregation of diblock copolymer chains.

Typical fitting results of the time dependence of I_E/I_M at a final φ_{water} of 0.5 are shown in Fig. 6. A triple exponential function is needed to fit the dynamic trace:

$$(I_\infty - I_t)/I_\infty = c_1 e^{-t/\tau_1} + c_2 e^{-t/\tau_2} + c_3 e^{-t/\tau_3}, \quad (3)$$

where c_1, c_2, and c_3 are the normalized amplitudes. τ_1, τ_2, and τ_3 are the characteristic relaxation time of three processes, and they are denoted $\tau_{1,fluo}$, $\tau_{2,fluo}$, and $\tau_{3,fluo}$, respectively ($\tau_{1,fluo} < \tau_{2,fluo} < \tau_{3,fluo}$). At a final φ_{water} of 0.5 and a copolymer concentration of 1.0 g/L, $\tau_{1,fluo}$, $\tau_{2,fluo}$, and $\tau_{3,fluo}$ are 0.008 s, 0.09 s, and 1.05 s, respectively.

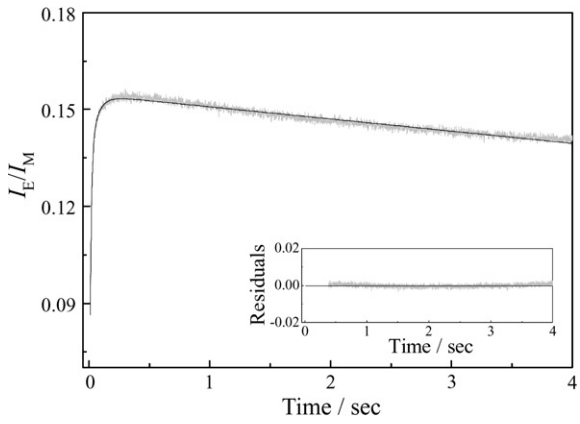

Fig. 6. Typical time dependence of I_E/I_M recorded during micelle formation. The curve was fitted by a triple-exponential function. The final *Py*-PNIPAM$_{50}$-*b*-POEGMA$_{18}$ diblock copolymer concentration was 1.0 g/L and φ_{water} was 0.5.

Both $\tau_{1,fluo}$ and $\tau_{2,fluo}$ exhibit positive amplitudes, while $\tau_{3,fluo}$ is a negative one. A comparison of the stopped-flow light fluorescence fitting results with those obtained from stopped-flow light scattering tells us $\tau_{1,scat}$ and $\tau_{2,scat}$ values agree fairly well with $\tau_{2,fluo}$ and $\tau_{3,fluo}$, suggesting that $\tau_{2,fluo}$ and $\tau_{3,fluo}$ can be ascribed to similar processes as those of $\tau_{1,scat}$ and $\tau_{2,scat}$. The ratio of amplitudes (c_1/c_2) for relaxation processes associated with $\tau_{1,fluo}$ and $\tau_{2,fluo}$ (Eq. (3)) is ~3/1, i.e., the fastest process ($\tau_{1,fluo} = 8$ ms) contributes ~75% of the initial increase of I_E/I_M. However, within comparable time scales, the scattered intensity only exhibits a relative increase of <4%. Thus, the newly detected $\tau_{1,fluo}$ (~8 ms) by stopped-flow fluorescence should be associated with the process of burst formation of small transient micelles, leading to the close contact between terminal pyrene groups and the appearance strong excimer emission peak [52].

Kositza et al. [25–27] studied the micellization dynamics of PEO$_{13}$-*b*-PPO$_{30}$-*b*-PEO$_{13}$ (Pluronic L64) block copolymer in aqueous solution using iodine laser temperature-jump (ILTJ) and stopped-flow techniques. Providing a small perturbation from the initial state, the ILTJ technique revealed that the characteristic relaxation time for the fastest process, unimer–micelle exchange, is in the range of 0.01–1 ms. In the current work, the stopped-flow technique monitored the unimer–micelle transition process. As the obtained first process possessed a characteristic relaxation time of ~8 ms, we cannot exclude the existence of even faster kinetic events at the early stage of micellization.

The relaxation from small transient micelles to quasi-equilibrium micelles can be detected by both stopped-flow fluorescence and light scattering techniques ($\tau_{1,scat}$ and $\tau_{2,fluo}$). During this process, the continuous increase of N_{agg} will lead to a more compact packing of copolymer chains, resulting in the further increase of I_E/I_M [45,53]. During the third process ($\tau_{2,scat}$ and $\tau_{3,fluo}$) associated with the relaxation into final equilibrium micelles, I_E/I_M decreases with time. This should be ascribed to the further dehydration and rearrangement of PNIPAM segments within the micelle core, restricting the mobility of pyrene end groups and their encountering probability [45]. Thus, the stopped-flow fluorescence technique can not only detect the initial burst formation of small transient micelles, but also probe the chain dynamics within the micelle core.

We further investigated the copolymer concentration effects on $\tau_{1,fluo}$, $\tau_{2,fluo}$, and $\tau_{3,fluo}$ at the final φ_{water} of 0.5, the triple exponential fitting results (Eq. (3)) are shown in Fig. 7. If the final polymer concentration is below 0.4 g/L, only a negative relaxation process is observed, indicating that the micelle size and/or number density of micelles are decreasing. For polymer concentrations >0.4 g/L, relaxation processes with positive amplitudes are

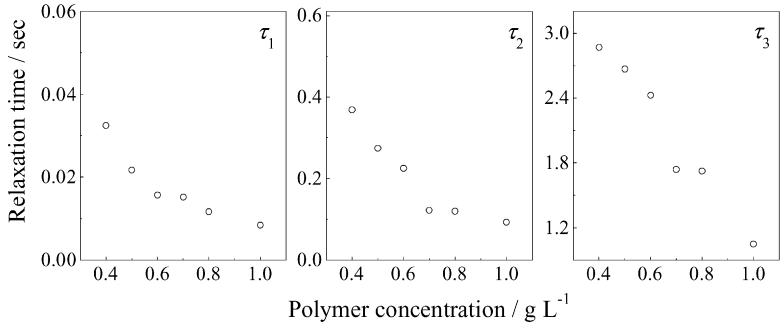

Fig. 7. Triple-exponential fitting results of the time-dependence of I_E/I_M during micelle formation at various *Py*-PNIPAM$_{50}$-*b*-POEGMA$_{18}$ concentrations. The experimental conditions were the same as those described in Fig. 6.

typically observed. $\tau_{1,\text{fluo}}$, $\tau_{2,\text{fluo}}$, and $\tau_{3,\text{fluo}}$ are in the range of 8–30 ms, 0.1–0.4 s, and 1.0–2.9 s, respectively. All of them decrease with increasing copolymer concentration.

The decrease of $\tau_{1,\text{fluo}}$ with increasing copolymer concentrations is quite understandable considering that the initial formation of small transient micelles mainly depends on the diffusion rate of unimer chains and their average spatial distances. The polymer concentration dependence of $\tau_{2,\text{fluo}}$ and $\tau_{3,\text{fluo}}$ follows similar trends to that of $\tau_{1,\text{scat}}$ and $\tau_{2,\text{scat}}$, suggesting that the micelle fusion/fission mechanism plays a key role during the growth from small transient micelles into quasi-equilibrium micelles and their relaxation into final equilibrium states [31,54,55].

4. Conclusion

Pyrene end-labeled diblock copolymer of *N*-isopropylacrylamide and oligo(ethylene glycol) methyl ether methacrylate, *Py*-PNIPAM-*b*-POEGMA, can molecularly dissolve in pure methanol or water, but forms PNIPAM-core micelles stabilized by soluble POEGMA blocks in an appropriate mixture of them. The cononsolvency-induced micellization kinetics of *Py*-PNIPAM-*b*-POEGMA was investigated via a combination of stopped-flow light-scattering and fluorescence techniques. Upon a stopped-flow jump of the volume fraction of water, φ_{water}, from 0 to the final range of 0.47–0.8, the time dependence of scattered light intensity and excimer-to-monomer fluorescence intensity ratio, I_E/I_M, were recorded. A comparison between the characteristic relaxation times obtained from both detection techniques revealed the presence of an intermediate stage during the cononsolvency-induced unimer-to-micelle transition, i.e., the burst formation of small transient micelles. To the best of our knowledge, this represents the first investigation of cononsolvency-induced micellization kinetics.

Acknowledgments

The financial supports of National Natural Scientific Foundation of China (NNSFC) Projects (20534020, 20674079, and 50425310), Specialized Research Fund for the Doctoral Program of Higher Education (SRFDP), and the Program for Changjiang Scholars and Innovative Research Team in University (PCSIRT) are gratefully acknowledged.

References

[1] G. Riess, Prog. Polym. Sci. 28 (2003) 1107–1170.
[2] T. Riley, S. Stolnik, C.R. Heald, C.D. Xiong, M.C. Garnett, L. Illum, S.S. Davis, S.C. Purkiss, R.J. Barlow, P.R. Gellert, Langmuir 17 (2001) 3168–3174.
[3] N.V. Semagina, A.V. Bykov, E.M. Sulman, V.G. Matveeva, S.N. Sidorov, L.V. Dubrovina, P.M. Valetsky, O.I. Kiselyova, A.R. Khokhlov, B. Stein, L.M. Bronstein, J. Mol. Catal. A: Chem. 208 (2004) 273–284.
[4] J.F. Gohy, S. Creutz, M. Garcia, B. Mahltig, M. Stamm, R. Jerome, Macromolecules 33 (2000) 6378–6387.
[5] G.E. Yu, A. Eisenberg, Macromolecules 31 (1998) 5546–5549.
[6] M. Moffitt, K. Khougaz, A. Eisenberg, Acc. Chem. Res. 29 (1996) 95–102.
[7] G.J. Liu, L.J. Qiao, A. Guo, Macromolecules 29 (1996) 5508–5510.
[8] J.J. Cornelissen, M. Fischer, N.A. Sommerdijk, R.J. Nolte, Science 280 (1998) 1427–1430.
[9] J.F. Ding, G.J. Liu, Macromolecules 30 (1997) 655–657.
[10] B.M. Discher, Y.Y. Won, D.S. Ege, J.C.M. Lee, F.S. Bates, D.E. Discher, D.A. Hammer, Science 284 (1999) 1143–1146.
[11] L.F. Zhang, A. Eisenberg, Science 268 (1995) 1728–1731.
[12] L.F. Zhang, A. Eisenberg, J. Am. Chem. Soc. 118 (1996) 3168–3181.
[13] S.Y. Liu, S.P. Armes, Langmuir 19 (2003) 4432–4438.
[14] V. Butun, N.C. Billingham, S.P. Armes, J. Am. Chem. Soc. 120 (1998) 11818–11819.
[15] C.D.H. Alarcon, S. Pennadam, C. Alexander, Chem. Soc. Rev. 34 (2005) 276–285.
[16] J. Rodriguez-Hernandez, F. Checot, Y. Gnanou, S. Lecommandoux, Prog. Polym. Sci. 30 (2005) 691–724.
[17] S.Y. Liu, N.C. Billingham, S.P. Armes, Angew. Chem., Int. Ed. 40 (2001) 2328–2331.
[18] J.V.M. Weaver, S.P. Armes, V. Butun, Chem. Commun. (2002) 2122–2123.
[19] H. Colfen, Macromol. Rapid Commun. 22 (2001) 219–252.
[20] A. Halperin, S. Alexander, Macromolecules 22 (1989) 2403–2412.
[21] E.A.G. Aniansson, S.N. Wall, M. Almgren, H. Hoffmann, I. Kielmann, W. Ulbricht, R. Zana, J. Lang, C. Tondre, J. Phys. Chem. 80 (1976) 905–922.
[22] E.A.G. Aniansson, S.N. Wall, J. Phys. Chem. 78 (1974) 1024–1032.
[23] E.A.G. Aniansson, S.N. Wall, J. Phys. Chem. 79 (1975) 857–858.
[24] I. Goldmints, F.K. von Gottberg, K.A. Smith, T.A. Hatton, Langmuir 13 (1997) 3659–3664.
[25] M.J. Kositza, C. Bohne, P. Alexandridis, T.A. Hatton, J.F. Holzwarth, Langmuir 15 (1999) 322–325.
[26] M.J. Kositza, C. Bohne, P. Alexandridis, T.A. Hatton, J.F. Holzwarth, Macromolecules 32 (1999) 5539–5551.
[27] M.J. Kositza, C. Bohne, T.A. Hatton, J.F. Holzwarth, Prog. Colloid Polym. Sci. 112 (1999) 146–151.
[28] G. Waton, B. Michels, R. Zana, Macromolecules 34 (2001) 907–910.
[29] Y.M. Wang, W.L. Mattice, D.H. Napper, Langmuir 9 (1993) 66–70.
[30] E.E. Dormidontova, Macromolecules 32 (1999) 7630–7644.
[31] F.J. Esselink, E. Dormidontova, G. Hadziioannou, Macromolecules 31 (1998) 2925–2932.
[32] F.J. Esselink, E.E. Dormidontova, G. Hadziioannou, Macromolecules 31 (1998) 4873–4878.
[33] I.A. Nyrkova, A.N. Semenov, Macromol. Theory Simul. 14 (2005) 569–585.
[34] I.A. Nyrkova, A.N. Semenov, Faraday Discuss. 128 (2005) 113–127.
[35] Z.Y. Zhu, S.P. Armes, S.Y. Liu, Macromolecules 38 (2005) 9803–9812.
[36] D. Wang, J. Yin, Z.Y. Zhu, Z.S. Ge, H.W. Liu, S.P. Armes, S.Y. Liu, Macromolecules 39 (2006) 7378–7385.
[37] J.Y. Rao, J. Xu, S.Z. Luo, S.Y. Liu, Langmuir 23 (2007) 11857–11865.
[38] F.M. Winnik, M.F. Ottaviani, S.H. Bossmann, M. Garciagaribay, N.J. Turro, Macromolecules 25 (1992) 6007–6017.
[39] H.G. Schild, M. Muthukumar, D.A. Tirrell, Macromolecules 24 (1991) 948–952.
[40] G.Z. Zhang, C. Wu, Phys. Rev. Lett. 86 (2001) 822–825.
[41] H.G. Schild, D.A. Tirrell, J. Phys. Chem. 94 (1990) 4352–4356.
[42] Z.S. Ge, Y.L. Cai, J. Yin, Z.Y. Zhu, J.Y. Rao, S.Y. Liu, Langmuir 23 (2007) 1114–1122.
[43] S. Picarra, J. Duhamel, A. Fedorov, J.M.G. Martinho, J. Phys. Chem. B 108 (2004) 12009–12015.
[44] S. Picarra, P. Relogio, C.A.M. Afonso, J.M.G. Martinho, J.P.S. Farinha, Macromolecules 37 (2004) 1670.
[45] F.M. Winnik, Macromolecules 23 (1990) 233–242.
[46] J.P.S. Farinha, S. Picarra, K. Miesel, J.M.G. Martinho, J. Phys. Chem. B 105 (2001) 10536–10545.
[47] S. Picarra, P.T. Gomes, J.M.G. Martinho, Macromolecules 33 (2000) 3947–3950.
[48] S. Picarra, J.M.G. Martinho, Macromolecules 34 (2001) 53–58.
[49] S. Picarra, E.J.N. Pereira, E.N. Bodunov, J.M.G. Martinho, Macromolecules 35 (2002) 6397–6403.

[50] S. Picarra, P. Relogio, C.A.M. Afonso, J.M.G. Martinho, J.P.S. Farinha, Macromolecules 36 (2003) 8119–8129.
[51] J.B. Birks, Photophysics of Aromatic Molecules, Wiley, New York, 1970.
[52] J.Y. Zhang, Y.T. Li, S.P. Armes, S.Y. Liu, J. Phys. Chem. B 111 (2007) 12111–12118.
[53] W. Chen, C.J. Durning, N.J. Turro, Macromolecules 32 (1999) 4151–4153.
[54] T. Haliloglu, I. Bahar, B. Erman, W.L. Mattice, Macromolecules 29 (1996) 4764–4771.
[55] A. Halperin, S. Alexander, Macromolecules 22 (1989) 2403–2412.